sustainability

Article

An MHD Flow of Non-Newtonian Fluid Due to a Porous Stretching/Shrinking Sheet with Mass Transfer

Ulavathi Shettar Mahabaleshwar [1], Thippeswamy Anusha [1], David Laroze [2], Nejla Mahjoub Said [3,4] and Mohsen Sharifpur [5,6,*]

1 Department of Mathematics, Davangere University, Shivagangotri, Davangere 577007, India; u.s.m@davangereuniversity.ac.in (U.S.M.); anushat.math@gmail.com (T.A.)
2 Instituto de Alta Investigación, CEDENNA, Universidad de Tarapacá, Casilla 7D, Arica 1000000, Chile; dlarozen@uta.cl
3 Department of Physics, College of Science, King Khalid University, Abha 61413, Saudi Arabia; nalmahjoub@kku.edu.sa
4 LGM, Preparatory Institute for Engineering Studies, University of Monastir, Monastir 5000, Tunisia
5 Department of Mechanical and Aeronautical Engineering, University of Pretoria, Pretoria 0002, South Africa
6 Department of Medical Research, China Medical University Hospital, China Medical University, Taichung 404, Taiwan
* Correspondence: mohsen.sharifpur@up.ac.za

Abstract: An examination is carried out for three-dimensional incompressible viscoelastic fluid flow over a porous stretching/shrinking sheet with hybrid nanoparticles copper-alumina $(Cu - Al_2O_3)$ in base fluid water (H_2O). The uniform magnetic field of strength B_0 is applied perpendicular to the fluid flow and considered the Navier slip. The mass transfer is considered with the chemical reaction rate. The governing equation for the defined flow forms the system of partial differential equations, which are then transformed into a system of ordinary differential equations via similarity transformations. The goal is to find the exact analytical solution, and the unique solution is determined by considering the boundary layer theory. Furthermore, the obtained system is solved to get the exact analytical solution for velocity and concentration fields in exponential form and in hypergeometric form, respectively. The exact solutions are obtained for velocity and temperature profiles, Skin friction, and Nusselt number. These findings are beneficial for future research in the present area. The parameters magnetic field, Inverse Darcy number, slip parameter, chemical reaction parameter, stretching/shrinking parameter, and viscoelastic parameter, influence the flow. The effect of these parameters on fluid velocity and concentration field will be analyzed through graphs. Skin friction and Nusselt number are also analyzed. This work found many applications in machining and manufacturing, solar energy, MHD flow meters and pumps, power generators, geothermal recovery, flow via filtering devices, chemical catalytic reactors, etc.

Keywords: viscoelastic fluid; hybridnanofluid; MHD; porosity; chemical reaction parameter

Citation: Mahabaleshwar, U.S.; Anusha, T.; Laroze, D.; Said, N.M.; Sharifpur, M. An MHD Flow of Non-Newtonian Fluid Due to a Porous Stretching/Shrinking Sheet with Mass Transfer. *Sustainability* **2022**, *14*, 7020. https://doi.org/10.3390/su14127020

Academic Editor: Fatih Selimefendigil

Received: 13 March 2022
Accepted: 1 June 2022
Published: 8 June 2022

1. Introduction

Mass transfer and momentum boundary layer flow have practical potential in the fields of polymer process and electrochemistry; the non-Newtonian fluids flow is a significant field in industry and so has become an field of interest for researchers. Several studies have been done on the flow of various non-Newtonian fluids [1,2].

Bhattacharya [3] studied the first order chemical reaction with the impact of mass transfer by using the shooting method. Akyildiz et al. [4] investigated the chemical reaction of non-Newtonian fluid through a porous medium to obtain an exact solution, which had some interesting properties that led to further study on chemically reactive species. Mahabaleshwar et al. [5,6] examined the inclined MHD flow, mass, and heat transfer with the effect of radiation and flow due to porous medium by considering different kinds of

BCs. Sarpkaya [7] discussed non-Newtonian fluids over a stretching sheet. The influence of viscous dissipation and chemical reaction on the stagnation point flow of NF due to the stretching/shrinking plate was examined by Murthy et al. [8]. The viscous flow on the shrinking sheet was examined by Miklavcic and Wang [9] and showed the existence and uniqueness, or non-uniqueness, of the exact solution. Due to the importance of the porous medium in practical applications, Mahabaleshwar et al. [10] examined the impact of both heat generation/absorption and stress work on the MHD flow due to a porous stretching sheet and analyzed the Brinkman model by considering the effect of slip on a shrinking sheet. Hayat et al. [11] gave attention to the flow of non-Newtonian fluid over a stretching/shrinking sheet and investigated the effect of partial slip. Rizwan et al. [12] studied the dual nature solution of the nanofluid convective flow in porous medium due to a shrinking sheet. Pop and Merkin et al. [13,14] studied unsteady flow in a porous medium considering the thermal slips using the shooting method and studied some limited cases. They continue work on finding a more exact solution to the same problem.

Knowing that the radiation effect is important for certain isothermal processes, Siddheshwar and Mahabaleshwar et al. [15] worked on the flow and heat transfer of MHD viscoelastic fluid flow on shrinking sheet under the effects of radiation. Turkyilmazoglu [16] also examined the flow, heat, and mass transfer of viscoelastic fluid and the impact of magnetic field and slip over a stretching surface and got multiple solutions. Furthermore, [17] examined heat and mass transfer of viscoelastic fluid due to a porous stretching sheet induced with a uniform magnetic field. Sakiadis [18] and Crane [19] are pioneers in the investigation of stretching sheet problems. An analytical study of Walters' liquid B over a stretching sheet has been discussed by Ghasemi [20]. Being motivated by these works, researchers conducted an investigation on stretching sheet problems. In the present work, there is investigation of the exact analytical solution for velocity and concentration field for 3D MHD flow viscoelastic HNF due to porous sheet which stretched/shrunk along both x and y axes with linear velocity and Navier slip. The mass transfer is analyzed with a chemical reaction rate parameter. The effects of different physical parameters on skin friction and Nusselt number are also analyzed.

2. Physical Model

Consider the 3D incompressible viscoelastic fluid flow with HNF due to porous stretching/shrinking sheet induced by uniform magnetic field of strength B_0, which is applied perpendicular to the fluid flow (Figure 1). The sheet is stretched/shrunk along the x-axis and the y-axis is perpendicular to it. The mass transfer is considered with chemical reaction rate k_C. The governing equations for the defined flow are as follows (Turkyilmazoglu [21]).

$$\frac{\partial u}{\partial x} + \frac{\partial v}{\partial y} + \frac{\partial w}{\partial z} = 0, \tag{1}$$

$$\begin{aligned} u\frac{\partial u}{\partial x} + \mathrm{v}\frac{\partial u}{\partial y} + w\frac{\partial u}{\partial z} &= \frac{\mu_{eff}}{\rho_{hnf}}\frac{\partial^2 u}{\partial z^2} + \gamma_0 u - \frac{\nu_{hnf}}{K^1}u - \frac{\sigma_{hnf}{B_0}^2}{\rho_{hnf}}u \\ &-k_0\left\{u\frac{\partial^3 u}{\partial x\partial z^2} + w\frac{\partial^3 u}{\partial z^3} - \left(\frac{\partial u}{\partial x}\frac{\partial^2 u}{\partial z^2} + \frac{\partial u}{\partial z}\frac{\partial^2 w}{\partial z^2} + 2\frac{\partial u}{\partial z}\frac{\partial^2 u}{\partial x\partial z} + 2\frac{\partial w}{\partial z}\frac{\partial^2 u}{\partial z^2}\right)\right\}, \end{aligned} \tag{2}$$

$$\begin{aligned} u\frac{\partial \mathrm{v}}{\partial x} + \mathrm{v}\frac{\partial \mathrm{v}}{\partial y} + w\frac{\partial \mathrm{v}}{\partial z} &= \frac{\mu_{eff}}{\rho_{hnf}}\frac{\partial^2 \mathrm{v}}{\partial z^2} + \gamma_0 \mathrm{v} - \frac{\nu_{hnf}}{K^1}\mathrm{v} - \frac{\sigma_{nf}{B_0}^2}{\rho_{nf}}\mathrm{v} \\ &-k_0\left\{\mathrm{v}\frac{\partial^3 \mathrm{v}}{\partial y\partial z^2} + w\frac{\partial^3 \mathrm{v}}{\partial z^3} - \left(\frac{\partial \mathrm{v}}{\partial y}\frac{\partial^2 \mathrm{v}}{\partial z^2} + \frac{\partial \mathrm{v}}{\partial z}\frac{\partial^2 w}{\partial z^2} + 2\frac{\partial \mathrm{v}}{\partial z}\frac{\partial^2 \mathrm{v}}{\partial y\partial z} + 2\frac{\partial w}{\partial z}\frac{\partial^2 \mathrm{v}}{\partial z^2}\right)\right\}, \end{aligned} \tag{3}$$

$$u\frac{\partial C}{\partial x} + \mathrm{v}\frac{\partial C}{\partial y} + w\frac{\partial C}{\partial z} = D_B\frac{\partial^2 C}{\partial y^2} + k_C(C - C_\infty), \tag{4}$$

with traditional BCs assumption,

$$\left.\begin{array}{l} u = ax + l\frac{\partial u}{\partial z},\ \mathrm{v} = by + l\frac{\partial \mathrm{v}}{\partial z},\ w = w_0,\ C = C_w,\ \text{at } z = 0, \\ u \to 0,\ \frac{\partial u}{\partial z} \to 0,\ \mathrm{v} \to 0,\ \frac{\partial \mathrm{v}}{\partial z} \to 0,\ C \to C_\infty \text{ as } z \to \infty \end{array}\right\}. \tag{5}$$

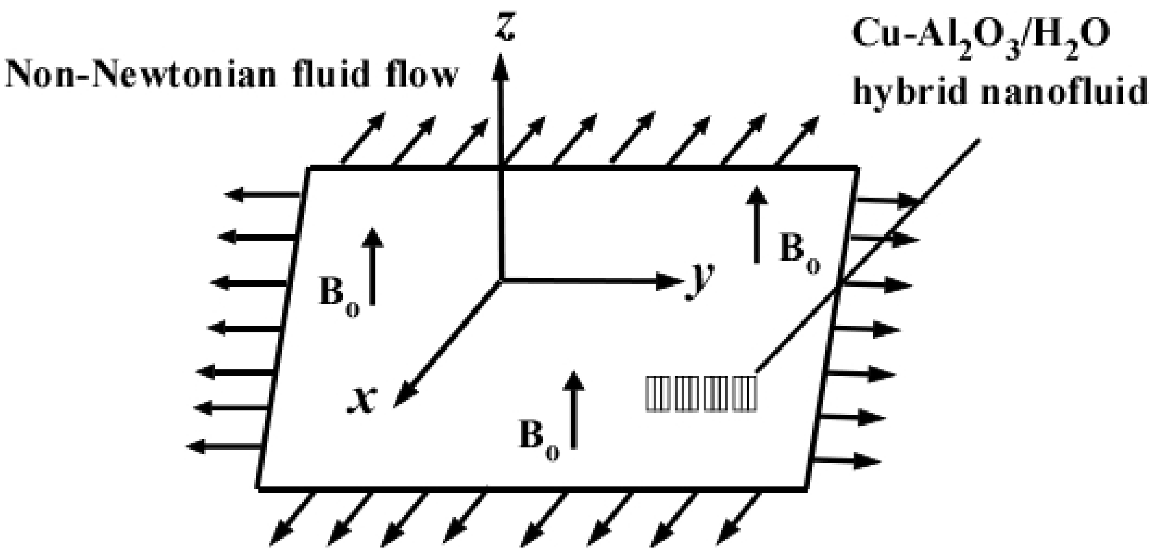

Figure 1. Schematic diagram of the flow.

Here, μ_{eff} is the effective viscosity, γ_0 is porosity, K^1 is permeability of porous medium, σ is electrical conductivity,k_C is the chemical reaction rate parameter, a and b are stretching rates along x and y axes, l is slip parameter.

The momentum equation for the velocity component w is neglected because of boundary layer limitations (Turkyilmazoglu [22]),

- The velocity in the axial direction is much larger than that in the transverse direction, i.e.,

$$u >> v >> w.$$

- The velocity gradient in the transverse direction is much bigger than the velocity gradient in the axial direction.

Now define the similarity transformations as follows,

$$u = |a|x\frac{\partial f}{\partial \eta},\ \mathrm{v} = |a|y\frac{\partial g}{\partial \eta},\ w = -\sqrt{|a|\nu}(f(\eta) + g(\eta)),\ \phi(\eta) = \frac{C - C_\infty}{C_w - C_\infty}$$

with

$$\eta = \sqrt{\frac{|a|}{\nu}}z, \tag{6}$$

Via these similarity transformations, the system PDEs in Equations (1)–(3) will transform into

$$\begin{aligned} &\tfrac{\Lambda}{\varepsilon_1} f_{\eta\eta\eta} + f_{\eta\eta}(f+g) - {f_\eta}^2 + \gamma f_\eta - \tfrac{1}{\varepsilon_1}\left(\varepsilon_2 Da^{-1} + \varepsilon_3 M\right) f_\eta \\ &\quad + K\left\{f_{\eta\eta\eta\eta}(f+g) + f_{\eta\eta}\left(f_{\eta\eta} - g_{\eta\eta}\right) - 2f_{\eta\eta\eta}\left(f_\eta + g_\eta\right)\right\} = 0 \end{aligned} \tag{7}$$

$$\begin{aligned} &\tfrac{\Lambda}{\varepsilon_1} g_{\eta\eta\eta} + g_{\eta\eta}(f+g) - {g_\eta}^2 + \gamma g_\eta - \tfrac{1}{\varepsilon_1}\left(\varepsilon_2 Da^{-1} + \varepsilon_3 M\right) g_\eta \\ &\quad + K\left\{g_{\eta\eta\eta\eta}(f+g) + g_{\eta\eta}\left(g_{\eta\eta} - f_{\eta\eta}\right) - 2g_{\eta\eta\eta}\left(f_\eta + g_\eta\right)\right\} = 0 \end{aligned} \tag{8}$$

$$\phi_{\eta\eta} + Sc(f+g)\phi_\eta + Sc\beta\phi = 0 \tag{9}$$

and the B.Cs (5) can be reduced as follows:

$$\begin{aligned} &f(0) = V_C,\ f_\eta(0) = d + \Gamma f_{\eta\eta}(0),\ g_\eta(0) = c + \Gamma g_{\eta\eta}(0),\ \phi(0) = 1, \\ &f_\eta(\infty) \to 0,\ f_{\eta\eta}(\infty) \to 0,\ g_\eta(\infty) \to 0,\ g_{\eta\eta}(\infty) \to 0,\ \phi(\infty) \to 0 \end{aligned} \tag{10}$$

Here, $\Lambda = \frac{\mu_{eff}}{\mu_f}$ is the Brinkman ratio, $Da^{-1} = \frac{\nu_f}{K^1|a|}$, is the inverse Darcy number, $M = \frac{\sigma_f {B_0}^2}{\rho_f|a|}$ is the magnetic parameter, $\gamma = \frac{\gamma_0}{|a|}$ is the porosity parameter, $K = \frac{k_0|a|}{\nu}$ is the viscoelastic parameter, $\Gamma = l\sqrt{\frac{|a|}{\nu}}$ is the first order velocity slip parameter, $V_C = -\frac{w_0}{\sqrt{|a|\nu}}$ indicates mass transpiration, where $V_C > 0$ for suction and $V_C < 0$ for injection, and $d = \frac{a}{|a|} = \pm 1$ and $c = \frac{b}{|a|}$ are the stretching/shrinking sheet parameters along the x and y axes, respectively, where $d = 1$ indicates stretching rate and $d = -1$ indicates shrinking rate. $\beta = \frac{k_C}{|a|}$ is the chemical reaction rate parameter.

The quantities $\delta_i' s,\ i = 1, 2, 3$ in Equation (7) are defined as

$$\delta_1 = \frac{\rho_{hnf}}{\rho_f},\ \ \delta_2 = \frac{\mu_{hnf}}{\mu_f},\ \ \delta_3 = \frac{\sigma_{nf}}{\sigma_f}. \tag{11}$$

2.1. Analytical Solution of Momentum Problem

The solutions of Equations (7) and (8) are assumed in the following form based on the analytical solutions taken as in Turkyilmazoglu [22] and Crane [19], with BCs as in Equation (10),

$$f(\eta) = V_C + \frac{d(1 - \exp(-\lambda\eta))}{\lambda(1 + \Gamma\lambda)}, g(\eta) = \frac{d(1 - \exp(-\lambda\eta))}{\lambda(1 + \Gamma\lambda)} \tag{12}$$

Using these solutions in Equation (7) will provide the following expressions,

$$\lambda = \frac{1}{\sqrt{2K}}, \tag{13}$$

$$-2d\left(1 + K\lambda^2\right) + (1 + \Gamma\lambda)\left\{\gamma - \frac{1}{\delta_1}\left(\delta_2 Da^{-1} + \delta_3 M\right) - \lambda\left(V_C - \frac{\Lambda}{\delta_1}\lambda + KV_C\lambda^2\right)\right\} = 0 \tag{14}$$

Using Equation (13) in Equation (14) will provide the expression for mass transpiration as

$$V_C = \frac{2\left[\frac{\Lambda}{\delta_1}\left(\sqrt{2K} + \Gamma\right) + 2K\Gamma\alpha + 2K\sqrt{2K}(-3d + \alpha)\right]}{3\left(2K + \Gamma\sqrt{2K}\right)} \tag{15}$$

where, $\alpha = \gamma - \frac{1}{\delta_1}\left(\delta_2 Da^{-1} + \delta_3 M\right)$ is assumed as one parameter which combines the effect of parameters, γ and $Da^{-1}, M > 0$. The physically interested parameters and local skin friction coefficient are given by

$$f_{\eta\eta}(0) = g_{\eta\eta}(0) = -\frac{\lambda d}{(1 + \Gamma\lambda)} \tag{16}$$

2.2. Analytical Solution of Mass Transfer Problem

To solve the Equation (9) with BCs in (10), the new variable is introduced as $\varepsilon = \frac{Sc}{\lambda^2}e^{-\lambda\eta}$ which will provide

$$\varepsilon\frac{\partial^2\phi}{\partial\varepsilon^2} + \left\{1 - Sc\chi_1 + \frac{2d}{1 + \Gamma\lambda}\varepsilon\right\}\frac{\partial\phi}{\partial\varepsilon} + \frac{Sc\beta}{\lambda^2}\frac{1}{\varepsilon}\phi = 0 \tag{17}$$

Here,

$$\chi_1 = \frac{V_C\lambda(1 + \Gamma\lambda) + 2d}{\lambda^2(1 + \Gamma\lambda)}$$

Next, the BCs (10) are reduced to become

$$\phi\left(\frac{Sc}{\lambda^2}\right) = 1,\ \ \phi(0) = 0, \tag{18}$$

where $\varepsilon = 0$ is the regular singular point of $\varepsilon = \frac{Sc}{\lambda^2}e^{-\lambda\eta}$. By assuming the solution of Equation (17) as power series solution $\phi(\varepsilon) = \sum_{r=0}^{\infty} c_r \varepsilon^{m+r}$ by adopting the Frobenius method (Hamid et al. [22]) the final solution in terms of ε can be obtained as

$$\phi(\varepsilon) = c_0 \varepsilon^{\chi_4} H[\chi_4, \chi_2 + 1, -\chi_3 \varepsilon] \tag{19}$$

The solution in terms of η will be

$$\phi(\eta) = c_0 \left(\frac{Sc}{\lambda^2} e^{-\lambda\eta}\right)^{\chi_4} H\left[\chi_4, \chi_2 + 1, -\chi_3 \frac{Sc}{\lambda^2} e^{-\lambda\eta}\right] \tag{20}$$

Using the BC the solution will be

$$\phi(\eta) = \left(e^{-\lambda\eta}\right)^{\chi_4} \frac{H\left[\chi_4, \chi_2 + 1, -\chi_3 \frac{Sc}{\lambda^2} e^{-\lambda\eta}\right]}{H\left[\chi_4, \chi_2 + 1, -\chi_3 \frac{Sc}{\lambda^2}\right]} \tag{21}$$

and the local Nusselt number is obtained as

$$-\phi_\eta(0) = \lambda\chi_4 - \frac{\chi_4}{\chi_2 + 1} \frac{\chi_3 Sc}{\lambda} \frac{H\left[\chi_4 + 1, \chi_2 + 2, -\chi_3 \frac{Sc}{\lambda^2}\right]}{H\left[\chi_4, \chi_2 + 1, -\chi_3 \frac{Sc}{\lambda^2}\right]} \tag{22}$$

Here,

$$\chi_2 = \sqrt{Sc^2 {\chi_1}^2 - 4\frac{Sc\beta}{\lambda^2}},\ \chi_3 = \frac{2\chi_2}{1 + \Gamma\lambda},\ \chi_4 = \frac{Sc\chi_1 + \chi_2}{2} \tag{23}$$

3. Results and Discussion

The 3D incompressible viscoelastic fluid flow over porous stretching/shrinking sheet with hybrid nanoparticlesis was examined along with the mass transfer problem by considering the impact of the chemical reaction rate. The uniform magnetic field of strength B_0 is applied to the flow. The governing equation for the defined flow Equations (1)–(4) with B.Cs (5) forms the system of PDEs which are then transformed to a system of ODE Equations (7)–(9) by applying similarity transformations as in Equation (6). Furthermore, the system of ODEs is solved to obtain the exact analytical solution for velocity and concentration fields in exponential form and in hypergeometric form, respectively. The new defined parameter $\alpha = \gamma - \frac{1}{\delta_1}\left(\delta_2 Da^{-1} + \delta_3 M\right)$, which includes the effect of magnetic field (M), Inverse Darcy number $\left(Da^{-1}\right)$, porosity parameter (γ), Brinkman ratio, (Λ) slip parameter (Γ), chemical reaction parameter (β), stretching/shrinking parameter (d), viscoelastic parameter (K), and Schmidt number (Sc), influences the flow. The effect of these parameters on fluid velocity and concentration field was analyzed through graphs. Skin friction and Nusselt number were also analyzed.The graphs are analyzed for HNF $Cu - Al_2O_3/H_2O$. The solid lines indicate $\Gamma = 0$ and the dotted lines indicate $\Gamma = 2$. The nanoparticle copper was noted to have higher rate of heat transfer and surface shear stress. To enhance the positive compatible features of each other, the appropriate composition of nanomaterials must be chosen. In previous studies, alumina has been a favorable nanoparticle due to its significant chemical motionlessness and stability.

Figures 2 and 3 depict the behavior of V_C with different parameters. Figure 2a,b demonstrates the solution curve of V_C verses K for stretching and shrinking sheet, respectively. The behavior of V_C for stretching and shrinking sheet are almost same, but solution in the shrinking case will shift upward. As the parameter α increases, V_C also increases in both the cases. It is clear that, for $\alpha < 0$, V_C will decrease as K increases and for $\alpha > 0$, V_C will increase as K increases. Furthermore, for $\alpha = 0$, V_C will decrease as K increases in the stretching case and V_C will increase as K increases in the shrinking case. Figure 3a,b show the solution domain of V_C verses Λ and d, respectively. As α increases the mass transpiration V_C also increases. Furthermore, V_C increases as Casson fluid parameter Λ increases and V_C decreases as d increases. V_C will be greater for higher values of the slip factor.

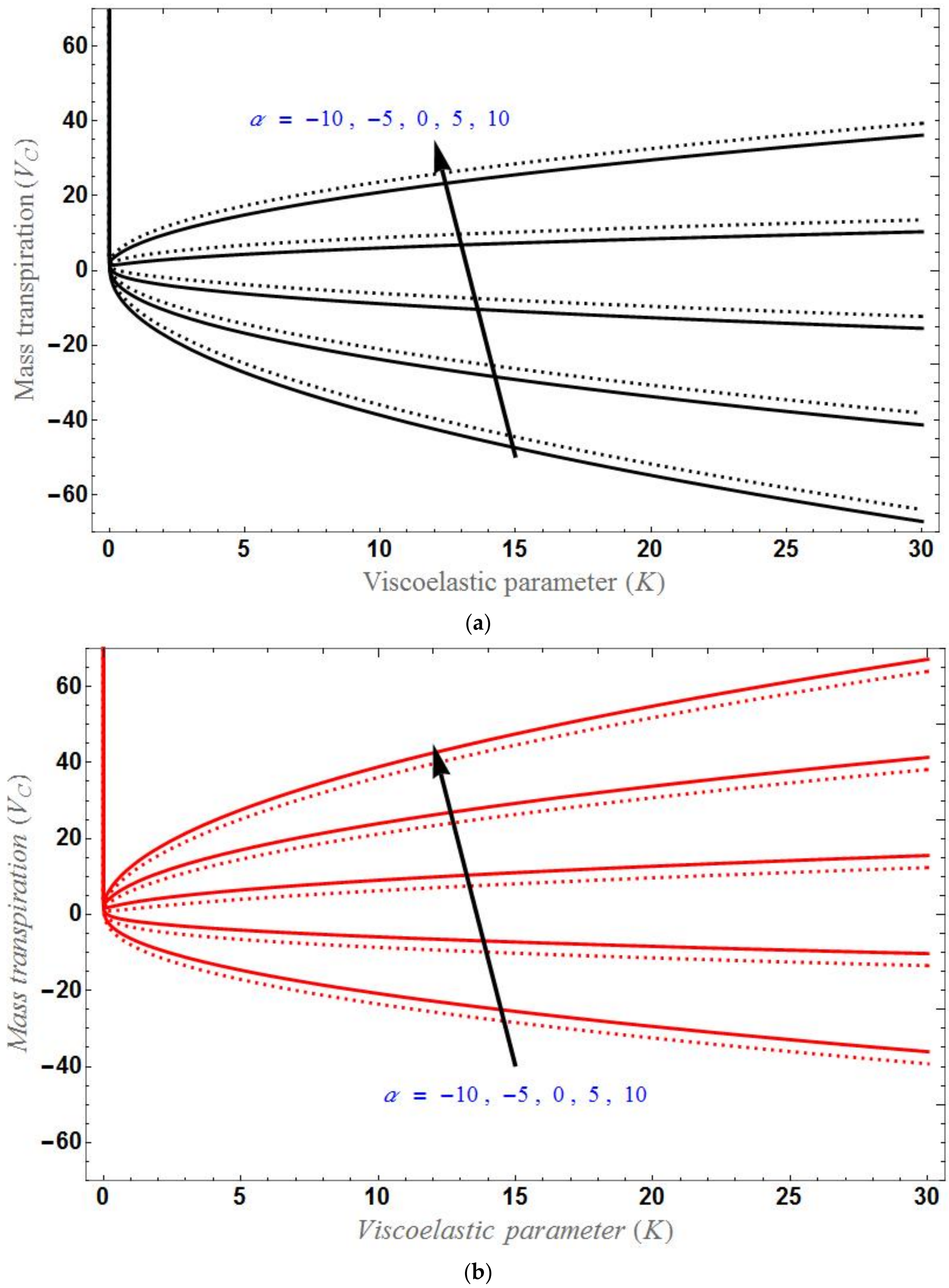

Figure 2. The solution domain of V_C versus K for different values of α in (**a**) stretching case $(d = 1)$ and (**b**) shrinking case $(d = -1)$.

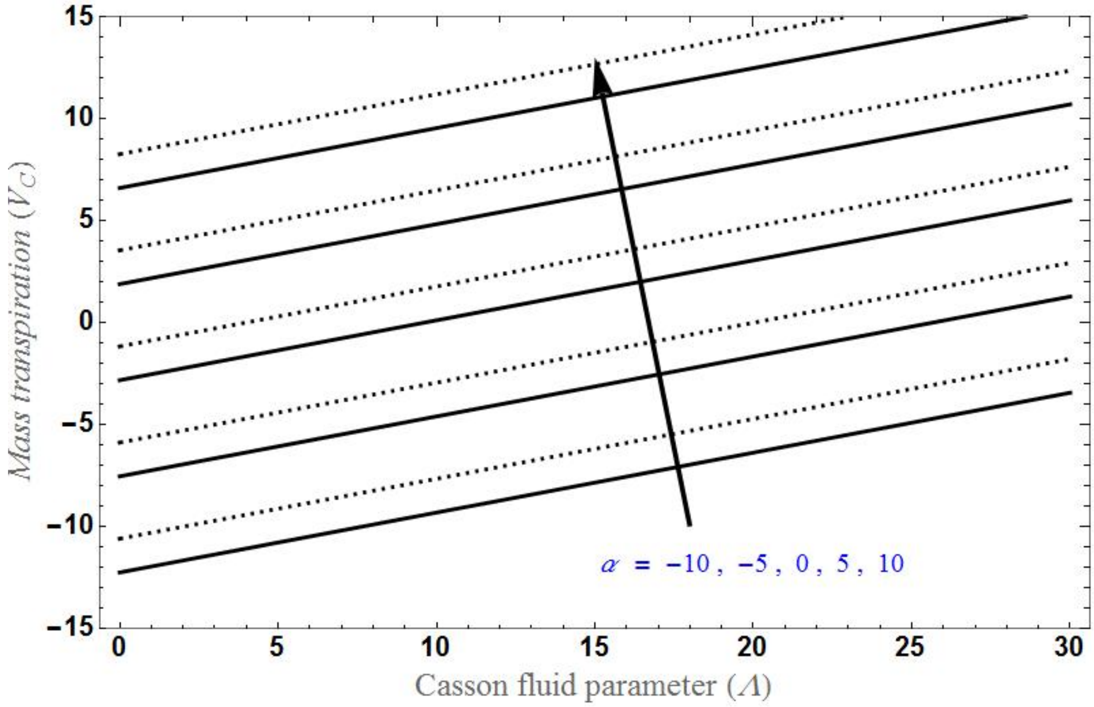

(**a**)

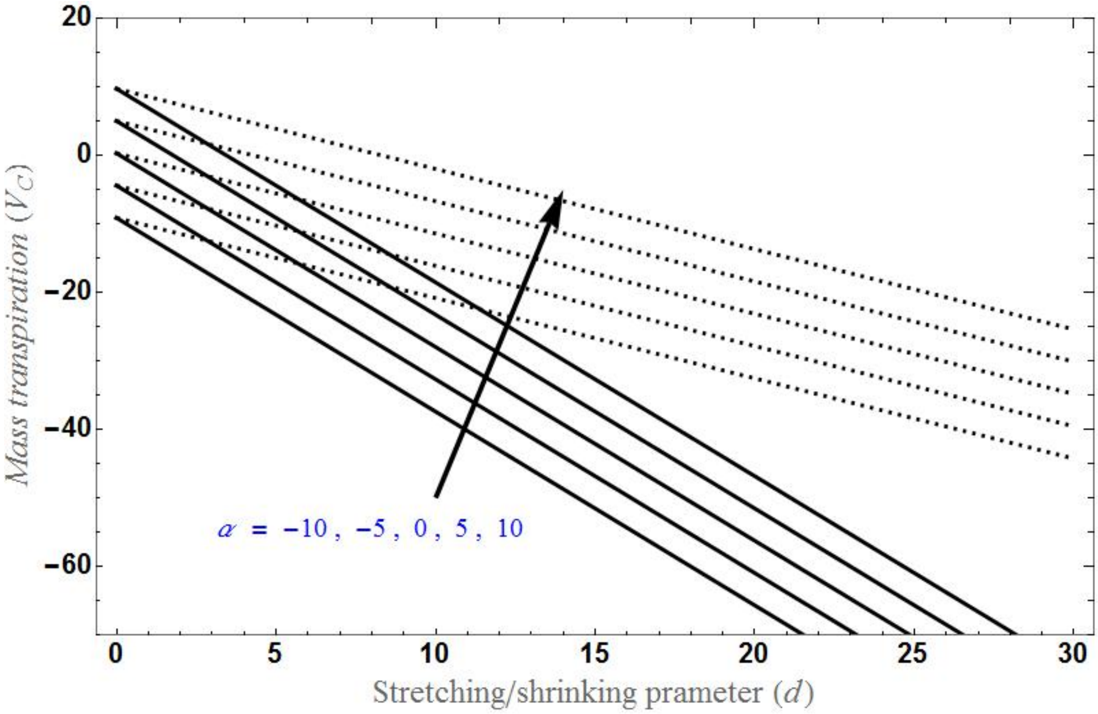

(**b**)

Figure 3. The solution domain of V_C for different values of α, (**a**) versus Λ and (**b**) versus d in stretching case.

Figure 4 depicts the transverse velocity for different values of α for both stretching and shrinking cases and increases with increases in α. Transverse velocity increases with increases in slip factor in the stretching case and decreases with increases in the slip factor in the shrinking case. Figure 5 demonstrates the axial velocity for various K, Γ, and d in both stretching and shrinking cases. Axial velocity increases with increases in K or d for the stretching case and decreases with increases in K or d for the shrinking case. In reverse, the axial velocity is lower for higher values of Γ in the stretching case and is higher for higher values of Γ in the shrinking case. Axial velocity decreases up to certain values of η, then becomes constant in the stretching case and continues increasing up to certain values of η, then becomes constant in the shrinking case.

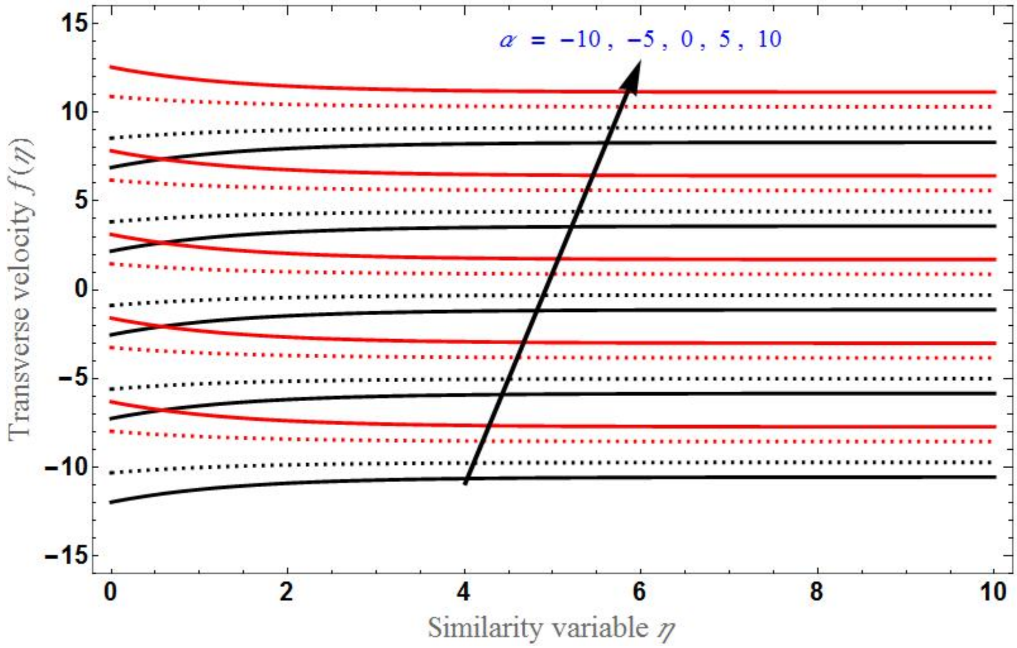

Figure 4. The transverse velocity $f(\eta)$ for different values of α. Black curves denote stretching case $(d = 1)$ and red curves denote shrinking case $(d = 1)$.

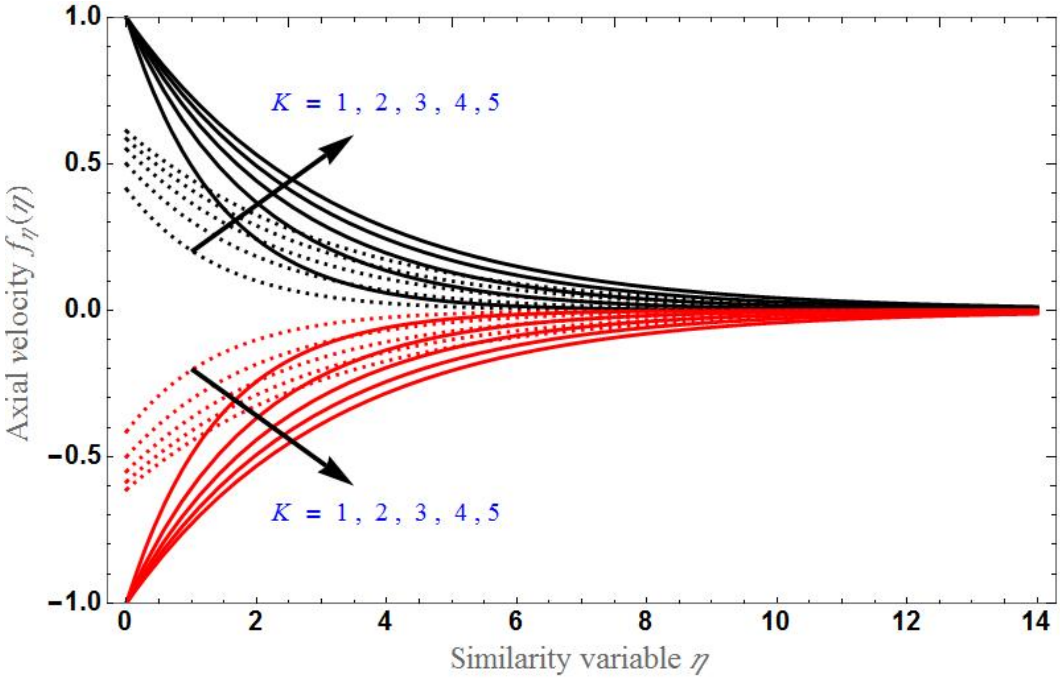

(**a**)

Figure 5. *Cont.*

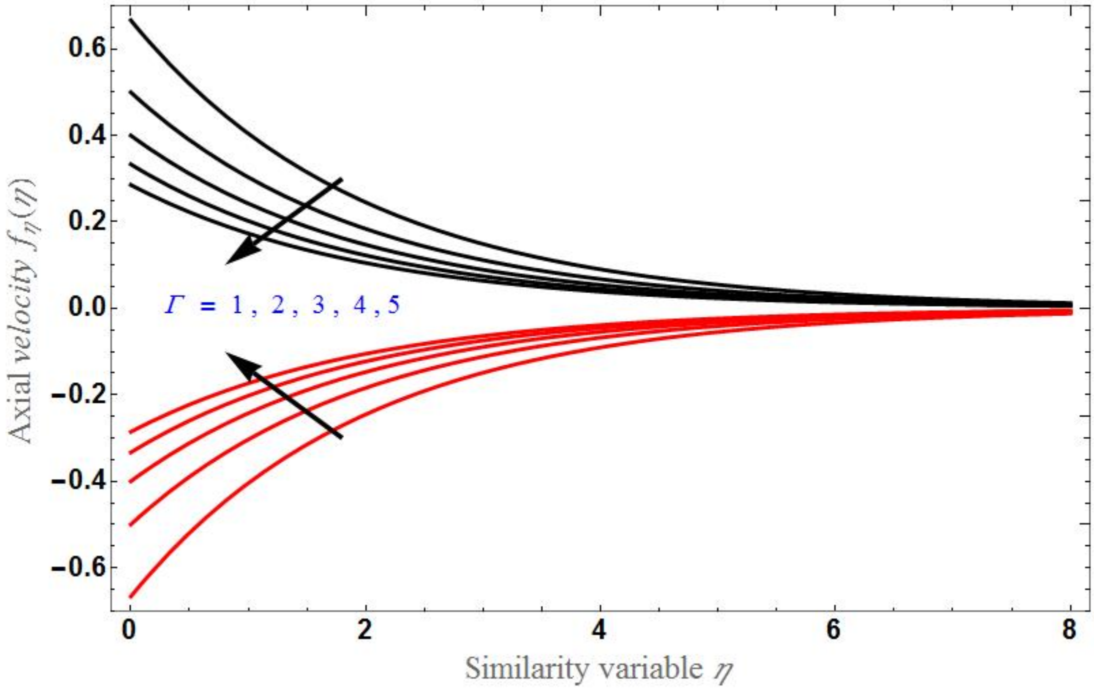

(**b**)

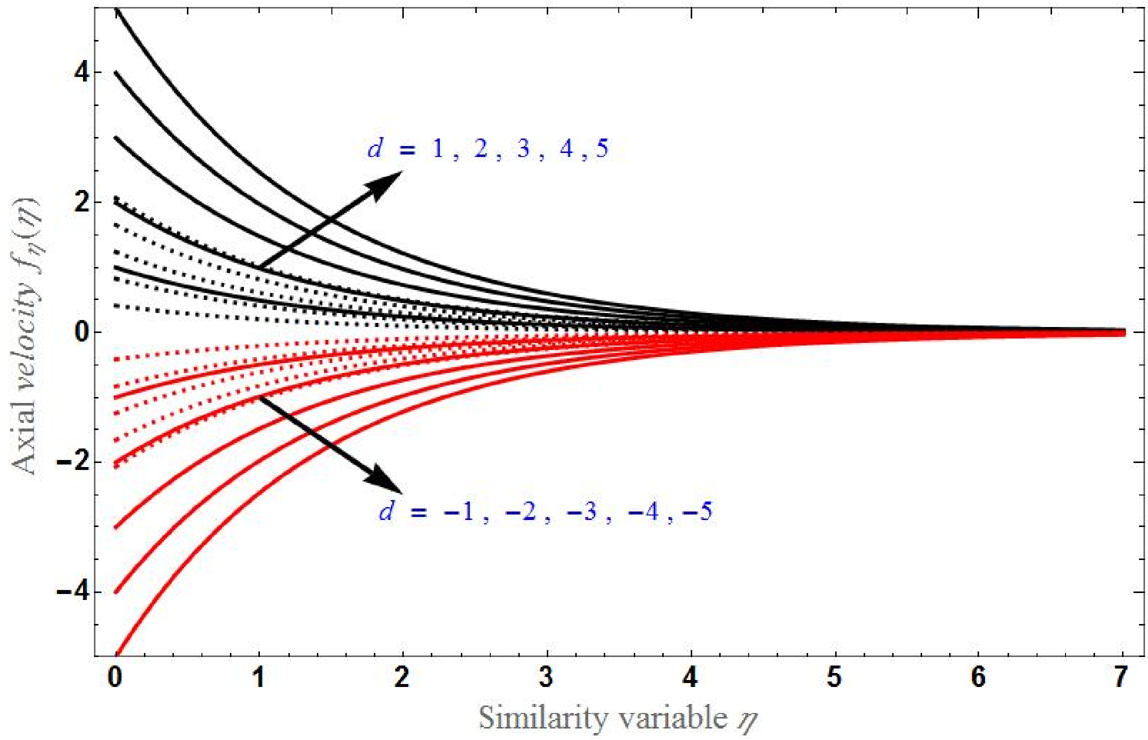

(**c**)

Figure 5. The axial velocity $f_\eta(\eta)$ for different values of K in (**a**), Γ in (**b**), and d in (**c**). Black curves denote the stretching case and red curves denote the shrinking case.

The behavior of skin friction with different parameters is analyzed in Figure 6. The effect of various values of d on skin friction versus K and versus Γ is demonstrated in Figure 6a,b, respectively, showing that skin friction is less for higher values of d. Furthermore, the skin friction is higher in the shrinking sheet case than in the stretching sheet case. Skin friction is increases with increases in K or Γ and becomes constant after a certain stage in the stretching case and will decrease with increases in K or Γ for the shrinking sheet case. It can also be observed in Figure 6c, which demonstrates the skin friction verses d for different values of K, where the stretching and shrinking cases are observed in the domains $0 < d \leq 10$ and $-10 \leq d < 0$, respectively. Skin friction decreases as d increases.

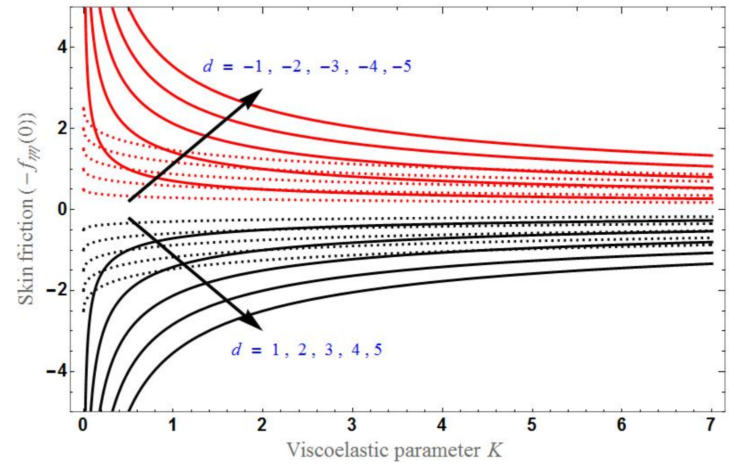

(**a**)

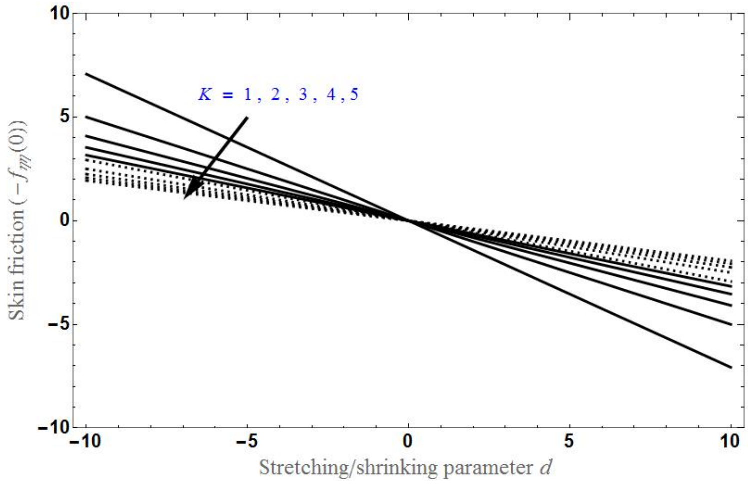

(**b**)

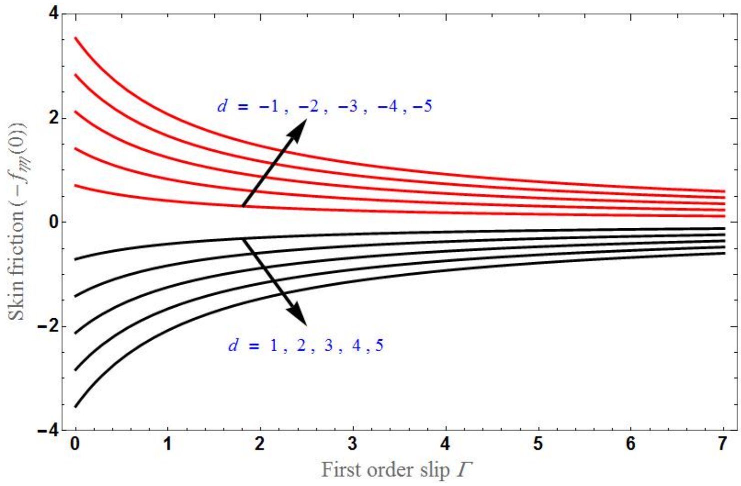

(**c**)

Figure 6. The skin friction $-f_{\eta\eta}(0)$, (**a**) verses K for different values of d, (**b**) verses d for different values of K, and (**c**) verses Γ for different values of d; black curves denote stretching case and red curves denote shrinking case.

Figures 7–9 demonstrated the concentration profile $\phi(\eta)$ by varying different parameters. The behavior of $\phi(\eta)$ according to the variation of K, β, and Γ for the stretching and shrinking cases is examined, respectively in Figures a and b. $\phi(\eta)$ will be higher for greater values of K or β. As seen earlier, $\phi(\eta)$ will be greater for higher values of Γ in the stretching case, and it will be less for higher values of Γ in the shrinking case. $\phi(\eta)$ decreases exponentially up to certain stage of η and after that becomes constant at zero.

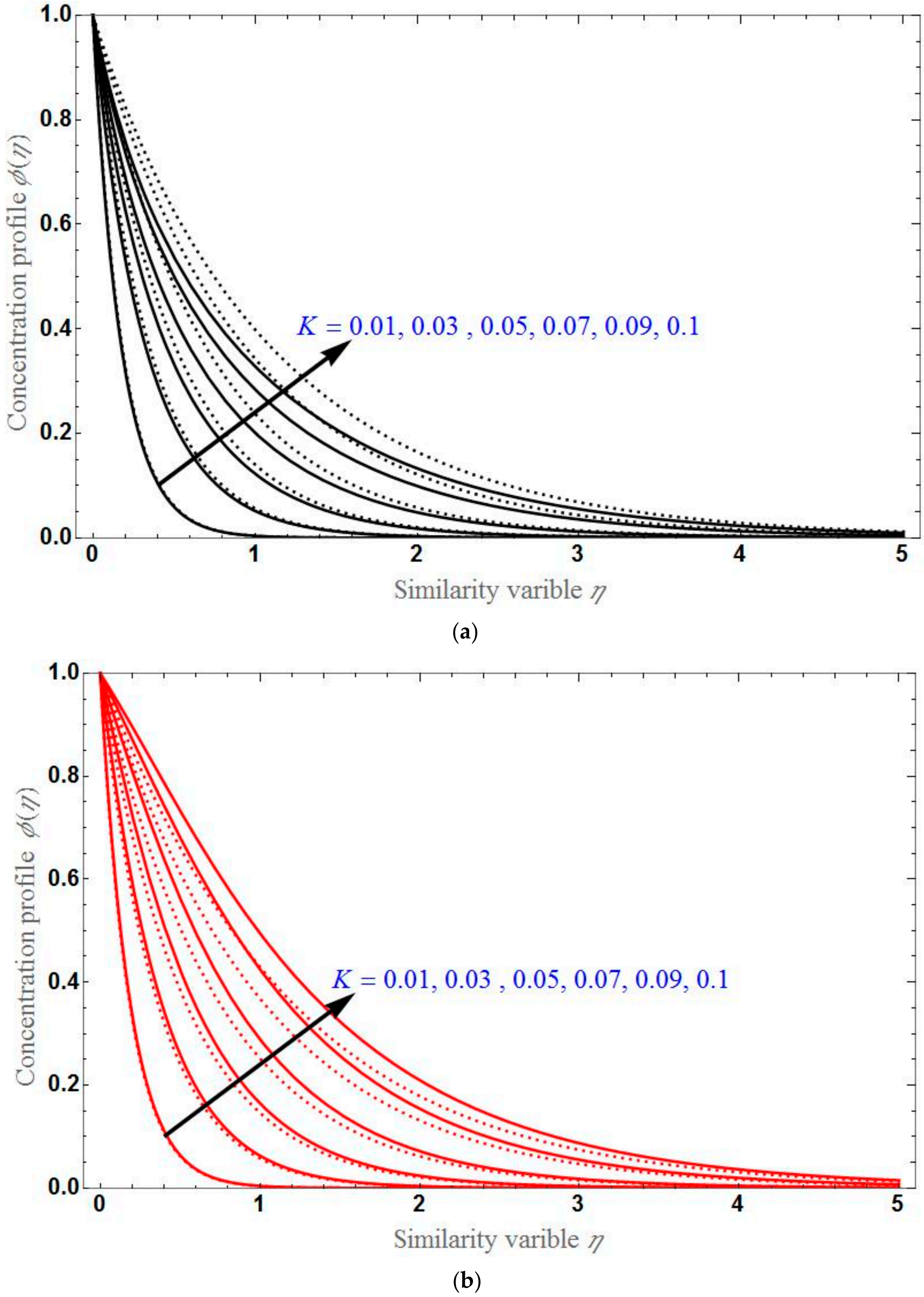

Figure 7. The concentration profile $\phi(\eta)$ for different values of K in (**a**) stretching case and in (**b**) shrinking case.

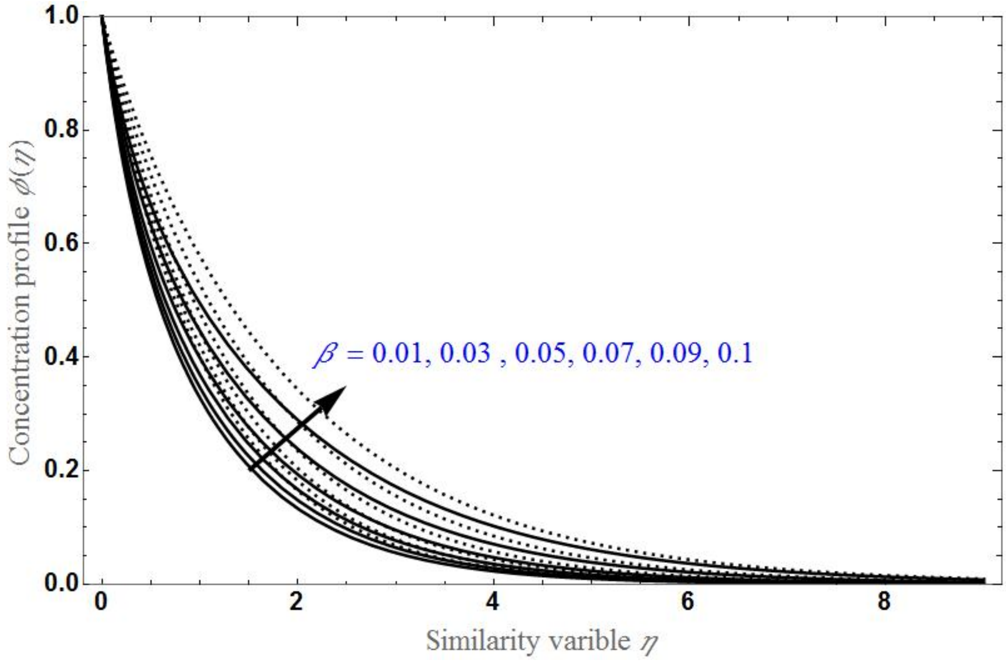

(**a**)

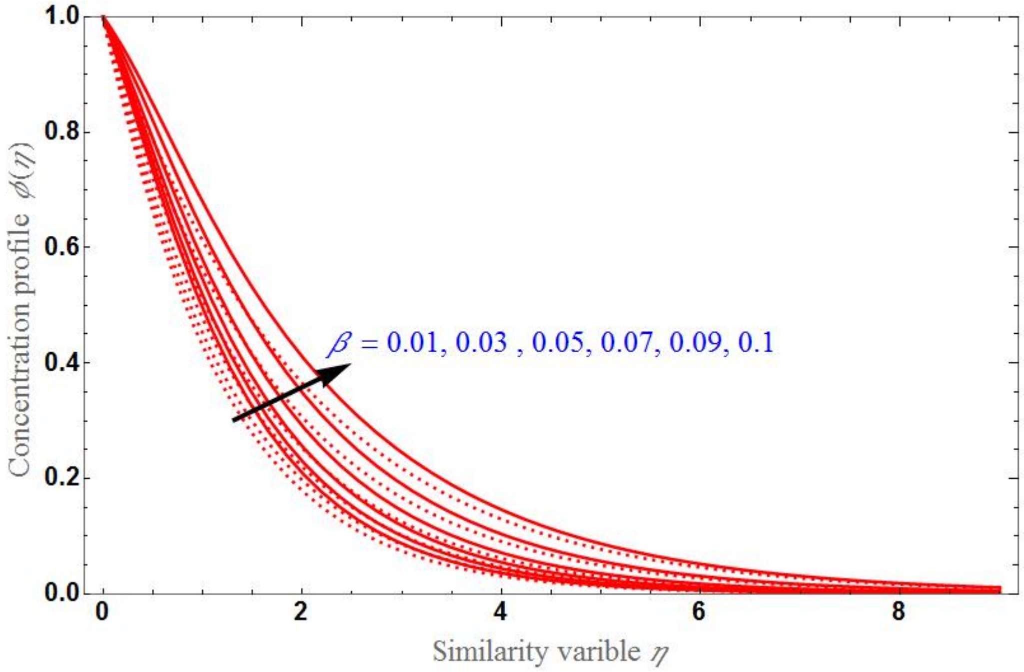

(**b**)

Figure 8. The concentration profile $\phi(\eta)$ for different values of β in (**a**) stretching case and in (**b**) shrinking case.

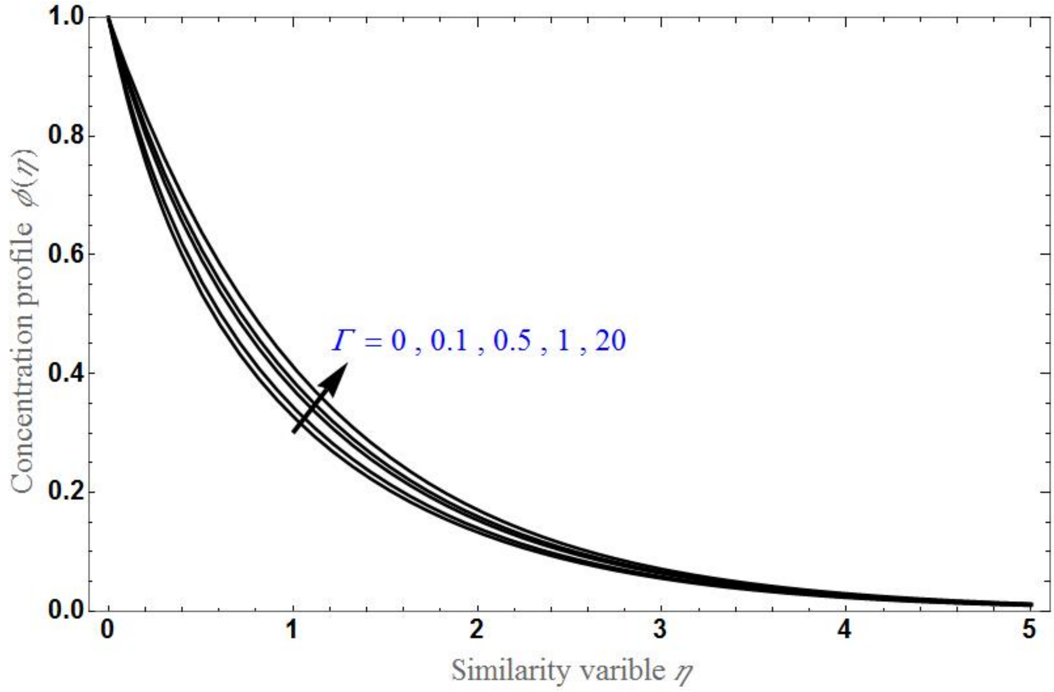

(**a**)

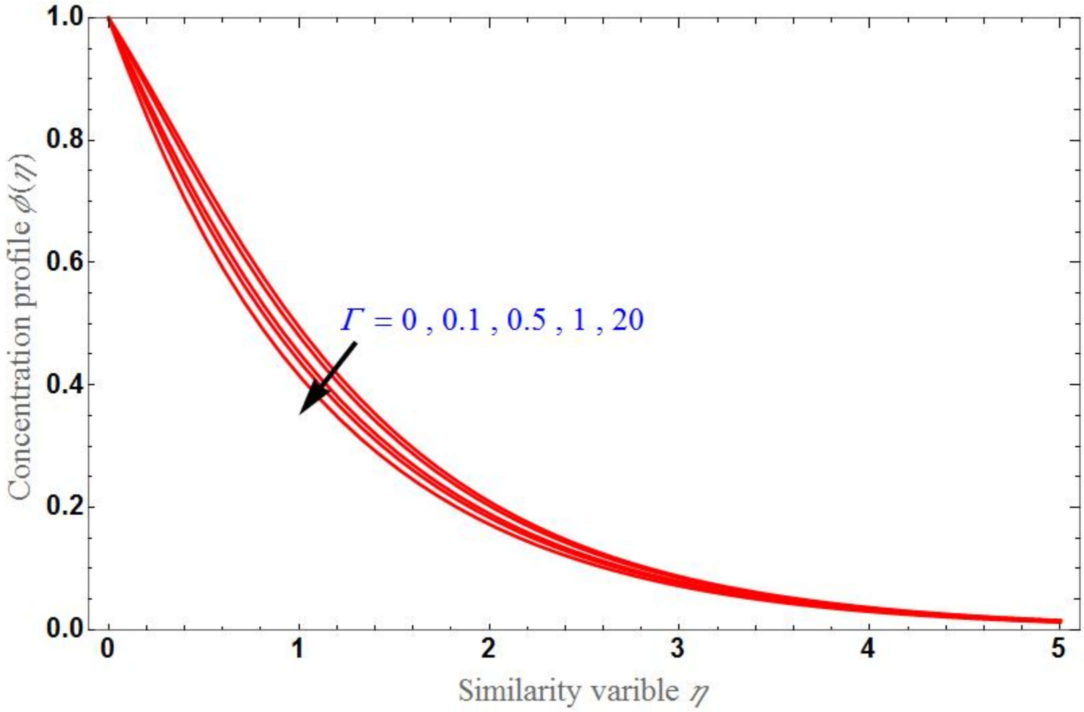

(**b**)

Figure 9. The concentration profile $\phi(\eta)$ for different values of Γ in (**a**) stretching case and in (**b**) shrinking case.

4. Conclusions

Consider the 3-dimensional incompressible viscoelastic fluid flow over the porous stretching/shrinking sheet with hybrid nanoparticles $Cu - Al_2O_3$ in base fluid H_2O. The uniform magnetic field of strength B_0 is applied perpendicular to the fluid flow and considered the Navier slip. The mass transfer is considered along with the chemical reaction rate. On converting a system of partial differential equations into system of ordinary differential equations via similarity transformations, it can be solved to get the exact analytical solution for velocity and concentration fields in exponential and hypergeometric forms, respectively. The parameters magnetic field, Inverse Darcy number, slip parameter, chemical reaction parameter, stretching/shrinking parameter, and viscoelastic parameter influence the flow. The effect of these parameters on fluid velocity and concentration field, skin friction and Nusselt number will be analyzed through graphs and the following observations can be made:

- As the parameter α increases, mass transpiration also increases in both the stretching and shrinking cases.
- Mass transpiration increases with increases in Casson fluid parameter Λ and slip factor, and will decreases as d increases.
- Transverse velocity will be higher for higher values of the slip factor in the stretching case and lower for higher values of the slip factor in the shrinking case.
- Axial velocity expands with K or d for the stretching case and shrinks with K or d for the shrinking case. The effect is reversed while varying Γ.
- Skin friction decreases with increases in d and it is greater in the shrinking sheet case than in the stretching sheet case.
- Skin friction increases with increases in K or Γ in the stretching case and will decrease with increases in K or Γ for the shrinking sheet case and become constant after a certain stage.
- The concentration profile will be higher for higher values of K or β; it will higher for higher values of Γ in the stretching case and lower for higher values of Γ in the shrinking case.

Author Contributions: Conceptualization, U.S.M. and T.A.; methodology, U.S.M.; software, U.S.M.; validation, D.L., N.M.S. and M.S.; formal analysis, U.S.M.; investigation, T.A.; resources, U.S.M.; data curation, D.L.; writing—original draft preparation, T.A.; writing—review and editing, M.S.; visualization, U.S.M.; supervision, U.S.M.; project administration, D.L.; funding acquisition, M.S. All authors have read and agreed to the published version of the manuscript.

Funding: Deanship of Scientific Research at King Khalid University, Saudi Arabia, through Large Groups (Project under grant number RGP.2/24/1443).

Data Availability Statement: No applicable for this paper.

Acknowledgments: The authors extend their appreciation to the Deanship of Scientific Research at King Khalid University, Saudi Arabia for funding this work through Large Groups (Project under grant number RGP.2/24/1443).

Conflicts of Interest: The authors declare no conflict of interest.

Nomenclature

Symbol	Description	S.I. Units
a, b	stretching/shrinking rates	$\left(s^{-1}\right)$
B_0	magnetic field strength	$\left(wm^{-2}\right)$
C	concentration field	$\left(mol/m^3\right) c, d$
c, d	Stretching/shrinking parameters along x and y axis	$(-)$
D_B	molecular diffusivity	$\left(m^2s^{-1}\right)$
Da^{-1}	Inverse Darcy number	$(-)$
k_0	material constant	(W/mK)
K	viscoelastic parameter	$\left(m^{-2}\right)$
k_C	chemical reaction parameter	$(-)$
K^1	permeability of porous medium	$\left(m^2\right)$
l	slip factor	$(-)$
Γ	first order slip parameter	$(-)$
M	magnetic parameter	$(-)$
Sc	Schmidt number	$(-)$
T	Temperature	(K)
V_C	Mass transpiration	$(-)$
(u, v, w)	velocities along x, y and z direction respectively	$\left(ms^{-1}\right)$
(x, y, z)	Cartesian coordinates	(m)
w_0	wall transpiration	$\left(ms^{-1}\right)$
Greek symbols		
β	chemical reaction parameter	$(-)$
η	Similarity variable	$(-)$
γ_0	porosity	$(-)$
γ	porosity parameter	$(-)$
μ	dynamic viscosity o	$\left(kgm^{-1}S^{-1}\right)$
ν	Kinematic viscosity	$\left(m^2s^{-1}\right)$
ρ	density	$\left(kgm^{-3}\right)$
ϕ	dimensionless concentration	$(-)$
σ	Electric conductivity	$\left(Sm^{-1}\right)$
Λ	Brinkman ratio	$(-)$
Subscripts		
hnf	Hybridnanofluid parameter	$(-)$
w	Wall condition	$(-)$
∞	ambient condition	$(-)$
Abbreviations		
HNF	hybrid nanofluid	$(-)$
MHD	Magneto hydrodynamics	$(-)$
ODEs	Ordinary differential equations	$(-)$
PDEs	Partial differential equations	$(-)$

References

1. Turkyilmazoglu, M. Magnetic field and slip effects on the flow and heat transfer of stagnation point Jeffrey fluid over deformable surfaces. *Z. Für Nat. A* **2016**, *71*, 549–556. [CrossRef]
2. Turkyilmazoglu, M.; Pop, I. Exact analytical solutions for the flow and heat transfer near the stagnation point on a stretching/shrinking sheet in a Jeffrey fluid. *Int. J. Heat Mass Transf.* **2013**, *57*, 82–88. [CrossRef]
3. Bhattacharyya, K. Dual solutions in boundary layer stagnation-point flow and mass transfer with chemical reaction past a stretching/shrinking sheet. *Int. Commun. Heat Mass Transf.* **2011**, *38*, 917–922. [CrossRef]
4. Akyildiz, F.T.; Bellout, H.; Vajravelu, K. Diffusion of chemically reactive species in a porous medium over a stretching sheet. *J. Math. Anal. Appl.* **2006**, *320*, 322–339. [CrossRef]
5. Mahabaleshwar, U.S.; Vinay Kumar, P.N.; Nagaraju, K.R.; Bognár, G.; Nayakar, S.N. A new exact solution for the flow of a fluid through porous media for a variety of boundary conditions. *Fluid* **2019**, *4*, 125. [CrossRef]
6. Mahabaleshwar, U.S.; Anusha, T.; Sakanaka, P.H.; Bhattacharyya, S. Impact of inclined Lorentz force and Schmidt number on chemically reactive Newtonian fluid flow on a stretchable surface when Stefan blowing and thermal radiation are significant. *Arab. J. Sci. Eng.* **2021**, *46*, 12427–12443. [CrossRef]
7. Sarpkaya, T. Flow of Non-Newtonian Fluids in a Magnetic Field. *Am. Inst. Chem. Eng.* **1961**, *7*, 324–328. [CrossRef]

8. Murthy, P.V.; RamReddy, C.; Chamkha, A.J.; Rashad, A.M. Significance of viscous dissipation and chemical reaction on convective transport in boundary layer stagnation point flow past a stretching/shrinking sheet in a nanofluid. *J. Nanofluids* **2015**, *4*, 214–222. [CrossRef]
9. Miklavcic, M.; Wang, C.Y. Viscous flow due to a shrinking sheet. *Q. Appl. Math.* **2006**, *2*, 283–290. [CrossRef]
10. Mahabaleshwar, U.S.; Lorenzini, G. Combined effect of heat source/sink and stress work on MHD Newtonian fluid flow over a stretching porous sheet. *Int. J. Heat Technol.* **2017**, *35*, S330–S335. [CrossRef]
11. Hayat, T.; Javed, T.; Abbas, Z. Slip flow and heat transfer of a second grade fluid past a stretching sheet through a porous space. *Int. J. Heat Mass Transf.* **2008**, *51*, 4528–4534. [CrossRef]
12. Haq, R.U.; Raza, A.; Algehyne, E.A.; Tlili, I. Dual nature study of convective heat transfer of nanofluid flow over a shrinking surface in a porous medium. *Int. Commun. Heat Mass Transf.* **2020**, *114*, 104583. [CrossRef]
13. Rohni, A.M.; Ahmad, S.; Pop, I.; Merkin, J.H. Unsteady mixed convection boundary-layer flow with suction and temperature slip effects near the stagnation point on a vertical permeable surface embedded in a porous medium. *Transp. Porous Media* **2012**, *92*, 1–14. [CrossRef]
14. Merkin, J.H.; Pop, I.; Rohni, A.M.; Ahmad, S. A further note on the unsteady mixed convection boundary layer in a porous medium with temperature slip: An exact solution. *Transp. Porous Media* **2012**, *95*, 373–375. [CrossRef]
15. Siddheshwar, P.G.; Mahabaleshwar, U.S. Effects of radiation and heat source on MHD flow of a viscoelastic liquid and heat transfer over a stretching sheet. *Int. J. Non-Linear Mech.* **2005**, *40*, 807–820. [CrossRef]
16. Turkyilmazoglu, M. Multiple analytic solutions of heat and mass transfer of magnetohydrodynamic slip flow for two types of viscoelastic fluids over a stretching surface. *J. Heat Transf.* **2012**, *134*, 071701. [CrossRef]
17. Khan, S.K.; Abel, M.S.; Sonth, R.M. Visco-elastic MHD flow, heat and mass transfer over a porous stretching sheet with dissipation of energy and stress work. *Heat Mass Transf.* **2003**, *40*, 47–57. [CrossRef]
18. Sakiadis, B.C. Boundary layer behavior on continuous solid surface. *Am. Inst. Chem. Eng.* **1961**, *7*, 26. [CrossRef]
19. Crane, L. Flow past a stretching plate. *Zeitschift Ange-Wandte Math. Phys.* **1970**, *21*, 645–647. [CrossRef]
20. Ghasemi, E.; Bayat, M.; Bayat, M. Viscoelastic MHD flow of Walters liquid B fluid and heat transfer over a non-isothermal stretching sheet. *Int. J. Phys. Sci.* **2011**, *6*, 5022–5039.
21. Turkyilmazoglu, M. Three dimensional MHD flow and heat transfer over a stretching/shrinking surface in a viscoelastic fluid with various physical effects. *Int. J. Heat Mass Transf.* **2014**, *78*, 150–155. [CrossRef]
22. Hamid, M.; Usman, M.; Khan, Z.H.; Ahmad, R.; Wang, W. Dual solutions and stability analysis of flow and heat transfer of Casson fluid over a stretching sheet. *Phys. Lett. A* **2019**, *383*, 2400–2408. [CrossRef]